www.nature.com/ismej

ISME

ARTICLE

Aerobic methylation of hydrogen sulfide to dimethylsulfide in diverse microorganisms and environments

Chun-Yang Li[1,5], Hai-Yan Cao[1,2,3,5✉], Qing Wang[2], Ornella Carrión[4], Xiaoyu Zhu[4], Jie Miao[2], Peng Wang[1,3], Xiu-Lan Chen[2,3], Jonathan D. Todd[4] and Yu-Zhong Zhang[1,2,3✉]

Dimethylsulfide (DMS) is the major biosulfur source emitted to the atmosphere with key roles in global sulfur cycling and potentially climate regulation. The main precursor of DMS is thought to be dimethylsulfoniopropionate. However, hydrogen sulfide (H_2S), a widely distributed and abundant volatile in natural environments, can be methylated to DMS. The microorganisms and the enzymes that convert H_2S to DMS, and their importance in global sulfur cycling were unknown. Here we demonstrate that the bacterial MddA enzyme, previously known as a methanethiol *S*-methyltransferase, could methylate inorganic H_2S to DMS. We determine key residues involved in MddA catalysis and propose the mechanism for H_2S *S*-methylation. These results enabled subsequent identification of functional MddA enzymes in abundant haloarchaea and a diverse range of algae, thus expanding the significance of MddA mediated H_2S methylation to other domains of life. Furthermore, we provide evidence for H_2S *S*-methylation being a detoxification strategy in microorganisms. The *mddA* gene was abundant in diverse environments including marine sediments, lake sediments, hydrothermal vents and soils. Thus, the significance of MddA-driven methylation of inorganic H_2S to global DMS production and sulfur cycling has likely been considerably underestimated.

The ISME Journal (2023) 17:1184–1193; https://doi.org/10.1038/s41396-023-01430-z

INTRODUCTION

Dimethylsulfide (DMS) is a volatile organic sulfur compound that plays important roles in chemotaxis [1], global sulfur cycling and climate regulation [2–4]. It is the major organosulfur compound emitted to the atmosphere, representing 20 Tg of sulfur annually [5, 6]. Atmospheric DMS oxidation products serve as cloud condensation nuclei and aerosols that influence the global radiation budget and climate [3, 4, 7].

The abundant marine osmolyte dimethylsulfoniopropionate (DMSP), produced by many phytoplankton and bacteria [8], is regarded as the major biosource of DMS [9] through the action of bacterial and algal DMSP lyase enzymes [9–12]. However, there are many DMSP-independent biopathways that generate DMS, for example, microbial cycling of *S*-methyl-methionine, dimethyl sulfoxide (DMSO) and methoxyaromatic compounds [13–15]. Furthermore, microorganisms in oxic and anoxic terrestrial and marine environments generate DMS from the methylation of methanethiol (MeSH) [16–18], a reactive volatile derived from DMSP demethylation [19] and/or hydrogen sulfide (H_2S) methylation [20, 21]. Many diverse bacteria (including cyanobacteria, *Proteobacteria* and *Actinobacteria*) which are abundant in sediment environments, contain the MeSH *S*-methyltransferase MddA [17, 18, 22], but the enzyme(s) responsible for H_2S methylation have not been identified.

H_2S is one of the Earth's most common and abundant volatile sulfur compounds [6, 23], often reaching several hundred micromolar and several millimolar concentrations in hydrothermal vents and marine sediment environments [24–26]. However, H_2S is toxic to cells because it inhibits cytochrome oxidase activity and blocks respiratory electron transport chains [27, 28]. Various H_2S detoxification pathways exist in living organisms [29, 30], including the methylation of H_2S to MeSH in higher animals and plants [29, 31]. Recently, a human thiol *S*-methyltransferase (METTL7B) was shown to catalyze H_2S *S*-methylation to DMS rather than MeSH [32]. Previous studies have also shown that bacteria in anoxic sediments *S*-methylate H_2S to DMS [20, 21], but to the best of our knowledge, H_2S methylation by aerobic bacteria has not been reported.

Here we evaluated the methylation of H_2S to DMS in various environmental samples, including seawater, marine and lake sediments, and soils, under oxic conditions. Furthermore, using *Neptunicoccus sediminis*, an aerobic *Rhodobacteraceae* bacterium isolated from marine sediment, as a model organism which converted H_2S to DMS, we established that its *mddA* gene, formerly only known to *S*-methylate MeSH [18], was responsible for this H_2S-dependent DMS production as a detoxification strategy. Biochemical analysis of the recombinant MddA confirmed its in vitro *S*-methylation of H_2S via MeSH to produce DMS and the kinetic feasibility. Based on sequence alignment, structure prediction, and site-directed mutagenesis, the putative catalytic mechanism of MddA was proposed, which enabled identification

[1]MOE Key Laboratory of Evolution and Marine Biodiversity, Frontiers Science Center for Deep Ocean Multispheres and Earth System & College of Marine Life Sciences, Ocean University of China, Qingdao, China. [2]State Key Laboratory of Microbial Technology, Marine Biotechnology Research Center, Shandong University, Qingdao, China. [3]Laboratory for Marine Biology and Biotechnology, Pilot National Laboratory for Marine Science and Technology, Qingdao, China. [4]School of Biological Sciences, University of East Anglia, Norwich Research Park, Norwich, UK. [5]These authors contributed equally: Chun-Yang Li, Hai-Yan Cao. ✉email: haiyancao92@126.com; zhangyz@sdu.edu.cn

Received: 4 February 2023 Revised: 27 April 2023 Accepted: 2 May 2023
Published online: 13 May 2023

of functional MddA enzymes in diverse *Archaea* and eukaryotic algae, not previously suspected of DMS production. Finally, bioinformatic analysis showed that *mddA* is widely distributed in diverse organisms and environments. Thus, H_2S-dependent DMS production may play an important, yet largely unappreciated role in microbial H_2S detoxification, global DMS emissions and sulfur cycling, and chemotaxis.

MATERIALS AND METHODS

Product analyses

Gas chromatography (GC) analyses were performed using a Nexis GC-2030 (Shimadzu, Japan) equipped with a flame photometric detector and a fused silica capillary column (30 m × 0.53 mm × 1 µm). The sample gas was injected into the GC using a purge-and-trap device. The carrier gas was nitrogen. The column temperature was 70 °C and the detector temperature was 250 °C. Standard curves for DMS were generated (using DMS standards from 0.1 nmol to 10 nmol) and used for quantification of DMS produced from sediment samples, bacterial cultures and enzyme reaction mixtures. The detecting lower limit of the method was 0.1 nmol. Volatile organic sulfur compounds were also determined by headspace GC-MS. The GC-MS analyses were performed using a Q Exactive GC Orbitrap GC-MS/MS System (Thermo Fisher Scientific, United States) equipped with a DB-5ms Ultra Inert GC column (Agilent Technologies, United States). All samples were analyzed in triplicate.

High performance liquid chromatography (HPLC) analyses were performed using an UltiMate 3000 (Thermo Fisher Scientific, United States) attached with a SunFire C_{18} reversed-phase column (4.6 × 250 mm, 5 µm particle size, Waters, United States). The detection wavelength was 260 nm, and injection volume was 10 µl. The samples were eluted with a linear gradient of 1–20% (v/v) acetonitrile in 50 mM ammonium acetate (pH 5.5) over 15 min at a flow rate of 1 ml/min. All samples were analyzed in triplicate. *S*-adenosyl-L-homocysteine (SAH) standard curves were established using SAH standards from 0.5 µM to 1 mM and used for quantitative detections. The detecting lower limit of the method was 5 pmol.

Assays of H_2S methylation by environmental samples and bacteria

Marine sediments were collected using a box corer from the East China Sea (30°00′ N, 124°00′ E and 31°30′ N, 123°30′ E) and the South China Sea (21°00′ N, 117°30′ E). Lake surface sediments were collected from the East Lake (30°33′ N, 114°22′ E). Soil samples were collected from garden soil (36°11′ N, 120°29′ E). Samples in the upper 10 cm were collected from each location and stored at −20 °C. Seawater samples were collected from the North Pacific Ocean (17°24′ N, 153°09′ E) at a depth of 30 meters and was filtered (every 5 L) through a 0.22 µm pore size polyethersulfone membrane (Millipore, United States).

The marine sediment and seawater samples were resuspended with artificial seawater which was prepared using sea salts (Sigma-Aldrich, United States) while the terrestrial samples were resuspended with distilled water. Then 1 ml resuspended mixture was added to a 10 ml sterile glass vial. The saturated H_2S aqueous solution (110 mM) was prepared by bubbling H_2S gas into water at 25 °C. Then H_2S solution was added to the vial to a final concentration of 1 mM. The vial was sealed immediately with aluminum crimp cap (molded polytetrafluoroethylene/butyl septa) using a manual crimper after the addition of H_2S, and incubated at 20 °C for 48 h. The same volume of distilled water instead of H_2S solution was used as the negative control. All operations were carried out under oxic conditions. GC was used for the detection of gaseous sulfur products as described above.

N. sediminis was cultured in Marine Broth 2216 medium (Becton, Dickinson and Company, United States) at 30 °C to an OD_{600} of 0.6. The cells were washed twice and resuspended with artificial seawater. Then 1 ml resuspended cells was transferred to a 10 ml sterile glass vial. H_2S solution was added to the culture to a final concentration of 1 mM and then the vial was sealed with aluminum crimp cap (molded polytetrafluoroethylene/butyl septa) immediately. The vials were incubated at 20 °C for 24 h without shaking. The products were also detected using GC.

Pseudomonas deceptionensis $M1^T$ wild-type and Δ*mddA* strains cultures on LB medium [33] were adjusted to an OD_{600} of 0.6. Cells were washed twice with M9 minimal medium [33] and inoculated into fresh M9 medium with 2 mM H_2S. After incubation at 30 °C, DMS generated from H_2S was quantified by GC as described [18]. DMS production rates are expressed as pmol mg protein^{-1} min^{-1}. The protein content in the cells was estimated by a Bradford method (BioRad, United States).

RT-qPCR analyses

N. sediminis was cultured in Marine Broth 2216 medium at 30 °C to an OD_{600} of 0.6. Then H_2S solution was added to the culture to a final concentration of 1 mM. The same volume of distilled water was added to the culture as the negative control. Samples were collected 2 h after the addition of different additives. Each sample for qPCR was performed in triplicate. Total RNA extraction was performed using RNeasy Kit (QIAGEN, Germany). Reverse transcription was performed using the PrimeScript RT Reagent Kit (TaKaRa, Japan). The RT-qPCR reaction was performed using LightCycler 480 II (Roche, Switzerland). Data were analyzed by the $2^{-\Delta\Delta Ct}$ method and *recA* was used was the reference gene. Significance was determined using paired two-tailed *t* test.

Genetic manipulations of *N. sediminis*

The knockout mutant Δ*mddA* of *N. sediminis* was constructed by homologous recombination. Two 1 kb DNA fragments, one upstream of *mddA* and one downstream of *mddA*, were amplified by PCR from its genomic DNA. The two DNA fragments were joined by overlapping PCR and cloned into plasmid pK18*mobsacB*-Ery [34]. The constructed vector was then conjugated into *N. sediminis* to generate Δ*mddA* mutant and Δ*mddA* mutants were confirmed by PCR and DNA sequencing, as described previously [34]. To complement the Δ*mddA* mutant, the *mddA* gene was amplified by PCR from *N. sediminis* genomic DNA and then cloned into plasmid pBBR1MCS-4 [35]. The constructed plasmid was conjugated into the Δ*mddA* mutant yielding the complemented strain Δ*mddA*/pBBR*mddA*. The primers used in this study are listed in Supplementary Table S1.

Protein expression and purification

All *mddA* genes were synthesized, codon optimized for expression in *E. coli*, by BGI Tech (China), and subcloned into the pET-22b vector to allow protein expression work with incorporation of a C-terminal hexahistidine tag. All site-directed mutations were introduced using QuikChange II mutagenesis kit (Agilent Technologies, United States) and were verified by sequencing. The expression plasmids were transformed into *E. coli* C43 (DE3) cells. Cells were grown in LB medium at 37 °C to an OD_{600} of 0.8. Then the culture was induced with 0.1 mM isopropyl-β-D-thiogalactopyranoside (IPTG) overnight at 20 °C. The cells were resuspended in a lysis buffer (50 mM Tris-HCl pH 8.0, 200 mM NaCl and 10% glycerol) and lysed using a high-pressure homogenizer. The lysate was centrifuged at 16,000 *g* for 20 min and the supernatant was then centrifuged at 200,000 *g* for 60 min to collect the membrane fraction. The membrane pellets were resuspended in lysis buffer containing 1.5% n-dodecyl-β-D-maltoside (DDM). After solubilization overnight at 4 °C, the mixture was centrifuged at 200,000 *g* for 30 min. The protein was purified using a Ni-nitriloacetic acid (Ni-NTA) agarose column followed by a size-exclusion chromatography column (Superdex 200, Cytiva, United States). The peak fractions were collected and stored at −80 °C.

Enzyme assays in vitro

Reaction mixtures (100 µl) contained 400 mM Tris-HCl (pH 8.0), 4 µg purified protein (or cell extract), 1 mM *S*-adenosyl-L-methionine (SAM) and 0.5 mM substrate (H_2S, MeSH, potassium iodide (KI), potassium thiocyanate (KSCN), dithiothreitol (DTT), captopril or D-penicillamine). For apparent optimum pH assays, H_2S was used as the substrate and Tris-HCl was replaced with Britton-Robinson buffer (20 mM final concentration). The reactions were carried out in 10 ml sterile glass vials. The vials were sealed immediately after the addition of the substrate. After incubation at 30 °C for 1 h, hydrochloric acid was injected to the reaction mixture to a final concentration of 0.1 M to terminate the reaction. The detection of gaseous DMS, MeSH and H_2S was performed by GC while the detection of non-volatile SAH and SAM was performed using HPLC.

For kinetic parameter assays, the reaction mixtures (100 µl) contained 400 mM Tris-HCl (pH 8.0), 4 µg purified *Pd*MddA, 20 mM SAM and varying concentrations of substrate (H_2S, MeSH or DTT). The reactions were performed as described above. The production of SAH by *Pd*MddA when using H_2S as the substrate was halved because it is a two-step methylation. Non-linear fitting of the data was performed using the Origin software.

Growth analyses of *N. sediminis* and *E. coli*

N. sediminis cells were cultured in Marine Broth 2216 medium at 30 °C for 48 h, washed and diluted 1/50 into fresh media for growth analysis. *E. coli* cells were cultured in LB medium at 37 °C overnight, washed and diluted 1/100 into fresh LB medium for growth analysis. H_2S (in solution) was added to the bacterial suspensions to a final concentration of 1 mM. The same volume of distilled water was added to the bacterial suspensions as negative controls. The bacterial suspensions with different additions were transferred to the wells in the microplate and then were incubated at 20 °C. The turbidity of the bacterial suspensions was measured at 600 nm using an FP-1100-C Automated Microbiology Growth Curve Analysis System (Bioscreen, Finland).

Bioinformatics analysis

The three-dimensional structure of *Pd*MddA was predicted using AlphaFold2 [36]. The structural data can be obtained from the AlphaFold Protein Structure Database [37] with accession code A0A0F6P9C0. The figures of the structure were generated with PyMOL (https://pymol.org/2/).

To explore the distribution of *mddA* gene in all domains, verified sequences of MddA were used as reference to extract homologs from public databases. For bacteria and archaea, MddA homologs were extracted from NCBI NR database by BLASTp with an e-value of 1e-30 and a minimum identity of 40%. Considering huge amount of hits were detected, these hits were further clustered at 80% amino acid identity and one representative sequence of each cluster was kept using CD-HIT [38]. For Eukaryotes, MddA homologs were extracted from re-assemblies of Marine Microbial Eukaryote Transcriptome Sequencing Project (MMETSP) (https://doi.org/10.5281/zenodo.740440) by hmmsearch with an e-value of 1e−30. To reduce false positives, only MddA sequences containing the catalytic histidine and five SAM binding residues were retained for tree building. Sequences alignment and trimming were respectively conducted by MAFFT [39] and TrimAl [40]. The tree was constructed using Maximum likelihood method in Fasttree [41]. Visualization of the tree was performed with iTOL [42].

The distribution of prokaryotic and eukaryotic *mddA* genes in global ocean was estimated in *Tara Oceans* datasets OM-RGC-v2 and MATOU, respectively. This analysis was conducted using the online webserver Ocean Gene Atlas [43] with hmmsearch (e-value < 1e−30) as the search method. Briefly, hmm databases based on the amino acid sequences of ratified *mddA* genes, two reference genes (DMSP lyase gene *alma1* for eukaryotic *mddA* and DMSP lyase gene *dddP* for prokaryotic *mddA*), and *recA* genes for normalization were submitted to Ocean Gene Atlas for searching homologs in OM-RGC-v2 metagenomes/metatranscriptomes and MATOU metagenomes/metatranscriptomes. For MATOU, only samples with a filter size within 0.8–20 µm (picoplankton/nanoplankton) were included in our analyses.

Environmental metagenomes analysis was conducted using the online webserver from the Integrated Microbial Genomes & Microbiomes (IMG/M) system [44]. The MddA, DddP and RecA sequences used to search the metagenomes are summarized in Supplementary Table S2. The metagenomes examined in this study are listed in Supplementary Table S3. The homologs of MddA, DddP and RecA in metagenomes of different environments with an e-value cut-off of 1e−30 and a minimum identity of 30% to reference sequences were extracted using BLASTP from IMG/M analysis system [44]. The abundance of *mddA* and *dddP* in metagenomes of different environments were calculated by using the numbers of unique MddA and DddP sequences normalized to the number of unique RecA sequences.

RESULTS

Microorganisms in diverse environments methylate H_2S to DMS

H_2S methylation to DMS is often prominent in anoxic sediments [20]; however, it is unclear whether H_2S is methylated to DMS in oxic environments. Considering H_2S is often abundant in marine sediments [24], we conducted oxic incubation experiments on East China Sea surface marine sediment to test for H_2S-dependent DMS production. GC analysis showed that DMS production under oxic conditions was stimulated by H_2S addition to the sediment, but no DMS was detected from heat-inactivated

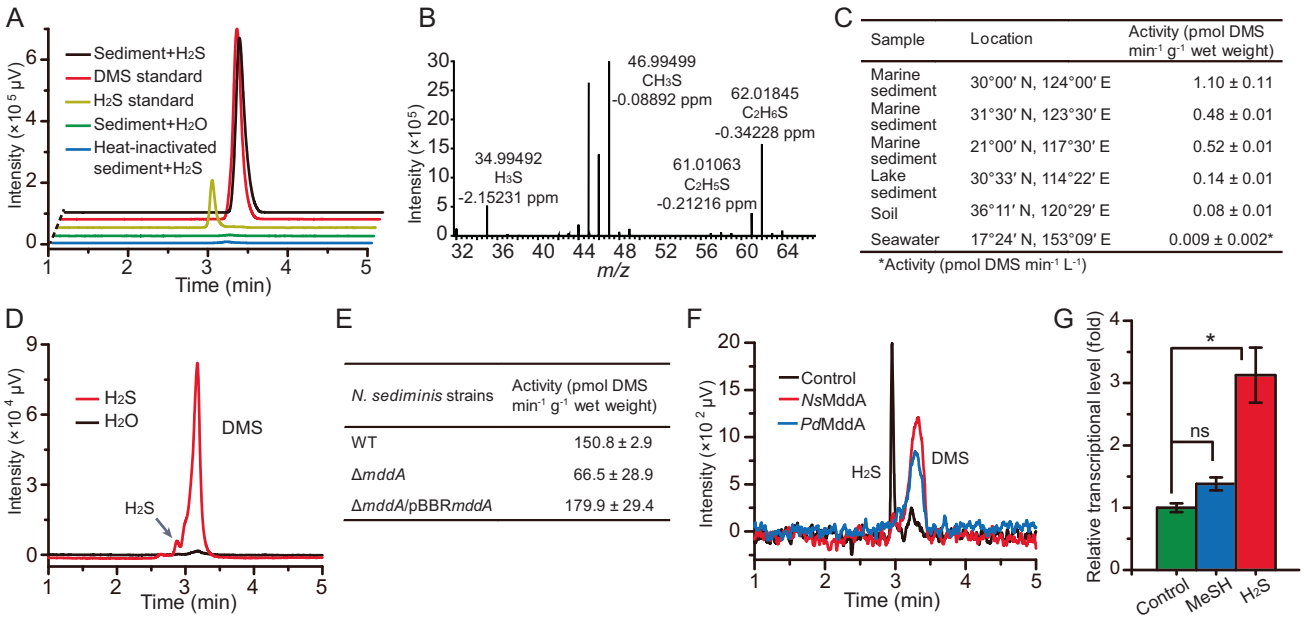

Fig. 1 Analyses of H_2S *S*-methylation by environmental samples and microorganisms. All experiments were conducted in triplicate. **A** GC analyses of the sulfur gases produced by marine sediment samples. Sediment samples were incubated with H_2S solution (1 mM final concentration) or H_2O (as the control). Heat-inactivated sediment was used as a microorganism-killed control. The major sulfur gas detected had the same retention time as the DMS standard. H_2S was not detected in the heat-inactivated samples, which have resulted from H_2S adsorption by the sediment. **B** GC-MS analysis of the sulfur gases liberated from the marine sediment in **A**. The fragment peaks showed that the main product was DMS. **C** H_2S-dependent DMS produced from diverse environmental samples. **D** GC analyses of *N. sediminis* cells incubated with H_2S solution (1 mM final concentration) or H_2O (control). **E** DMS produced from H_2S by *N. sediminis* wild-type and mutant strains. **F** In vitro SAM-dependent *S*-methylation of H_2S activities of cell extracts of *E. coli* expressing the *Ns*MddA and *Pd*MddA. H_2S was added to the mixture and DMS was produced. Cell extract of *E. coli* with empty pET-22b vector was used as negative control. **G** RT-qPCR analyses of *NsmddA* in *N. sediminis*. *NsmddA* gene transcription was significantly enhanced by growth in the presence of H_2S, and not MeSH. ns not significant. *$p < 0.05$ (paired two-tailed *t* test).

samples (Fig. 1A, B), suggesting that DMS formation from H_2S was mediated by microorganisms. No MeSH was detected in these incubations, indicating that if MeSH was an intermediate in H_2S-dependent DMS production it did not accumulate and was likely quickly *S*-methylated to DMS or lost to biotic and/or abiotic oxidative processes.

To investigate the potential for H_2S-dependent DMS production in more diverse oxic environments, we collected various environmental samples, including marine surface sediment, seawater, lake surface sediment, and soil, and incubated them with H_2S under oxic conditions (see methods). All these samples generated DMS at 0.08–1.10 pmol DMS min^{-1} g^{-1} wet weight (0.009 pmol DMS min^{-1} L^{-1} for the seawater sample) (Fig. 1C), implying that oxic H_2S-dependent DMS production occurs in diverse oxic environments when H_2S is present. The observed DMS production rates varied in the diverse oxic samples, but the marine sediments produced more DMS than those from terrestrial samples.

N. sediminis *S*-methylates H_2S to DMS

Bacteria isolated from marine sediment samples were screened for H_2S-dependent DMS production to identify model bacteria with this ability. Of these isolates, *N. sediminis*, an aerobic *Rhodobacteraceae* member originally isolated from Yellow Sea sediment [45], methylated H_2S to produce DMS at a rate of 150.8 pmol DMS min^{-1} g^{-1} wet weight under oxic conditions (Fig. 1D, E). No MeSH was detected in these incubations of *N. sediminis* with H_2S (Fig. 1D), which was consistent with the sediment incubations described above.

Identification of a key enzyme driving H_2S-dependent DMS production

The conversion of H_2S to DMS is a methyl transfer reaction, and we postulated that a thiol (R-SH) *S*-methyltransferase (EC 2.1.1.9) was likely involved. To identify the methyltransferases catalyzing the conversion of H_2S to DMS in *N. sediminis*, its genome was analyzed for candidate methyltransferases homologous to those known to methylate H_2S [31, 32, 46] or other thiol *S*-methyltransferases (Supplementary Table S4). This analysis only identified a candidate MeSH *S*-methyltransferase MddA protein in *N. sediminis* (*Ns*MddA, WP_069301345.1) with 46% amino acid identity to *P. deceptionensis* $M1^T$ MddA (*Pd*MddA, WP_048359798.1), which *S*-methylates MeSH to DMS but was previously reported to lack the ability to *S*-methylate H_2S [18].

We next investigated whether the putative *Ns*MddA was involved in H_2S-dependent DMS production. The results showed that *E. coli* cell extracts expressing cloned *NsmddA* showed in vitro SAM-dependent DMS production from H_2S (Fig. 1F), indicating that *Ns*MddA likely *S*-methylates H_2S to MeSH and then MeSH to DMS. In addition, *Pd*MddA also showed in vitro SAM-dependent DMS production from H_2S in *E. coli* extracts (Fig. 1F) under the conditions used here, which contradicted the previous work done on this protein [18]. To confirm that MddA was responsible for in vivo H_2S-dependent methylation, ultimately generating DMS, we constructed a *N. sediminis* Δ*mddA* knock out mutant, and analyzed its ability to *S*-methylate H_2S along with the *P. deceptionensis* Δ*mddA* mutant [18]. H_2S-dependent DMS production was ~2-fold reduced in the *N. sediminis* Δ*mddA* strain compared to the wild type *N. sediminis* strain, with this reduction in activity being fully restored to wild type levels by cloned *Ns*MddA (Fig. 1E). Furthermore, H_2S-dependent DMS production was abolished in the *P. deceptionensis* Δ*mddA* mutant (Supplementary Table S5). These data indicate that *mddA* in *N. sediminis* and *P. deceptionensis* encode a functional H_2S *S*-methyltransferase that generates DMS via MeSH, but also that *N. sediminis* likely contains another unidentified H_2S *S*-methyltransferase. This is consistent with previous research, in which diverse isolated bacteria had Mdd activity but lacked *mddA* in their genomes [17, 22]. The transcription of *NsmddA* was upregulated 3-fold when *N. sediminis* was grown with H_2S, but not with MeSH (Fig. 1G), likely explaining the induction of DMS production seen in oxic sediment and water incubation experiments when H_2S was added.

Characterization of the MddA enzyme

When expressed and purified from *E. coli*, the *Ns*MddA protein was unstable and readily precipitated. Thus, the *Pd*MddA, which was more stable when purified from *E. coli*, was used as the model protein to examine the enzymology of MddA. The *Pd*MddA was shown to have in vitro SAM-dependent H_2S and MeSH *S*-methyltransferase activity yielding SAH and DMS (Fig. 2A–E). In

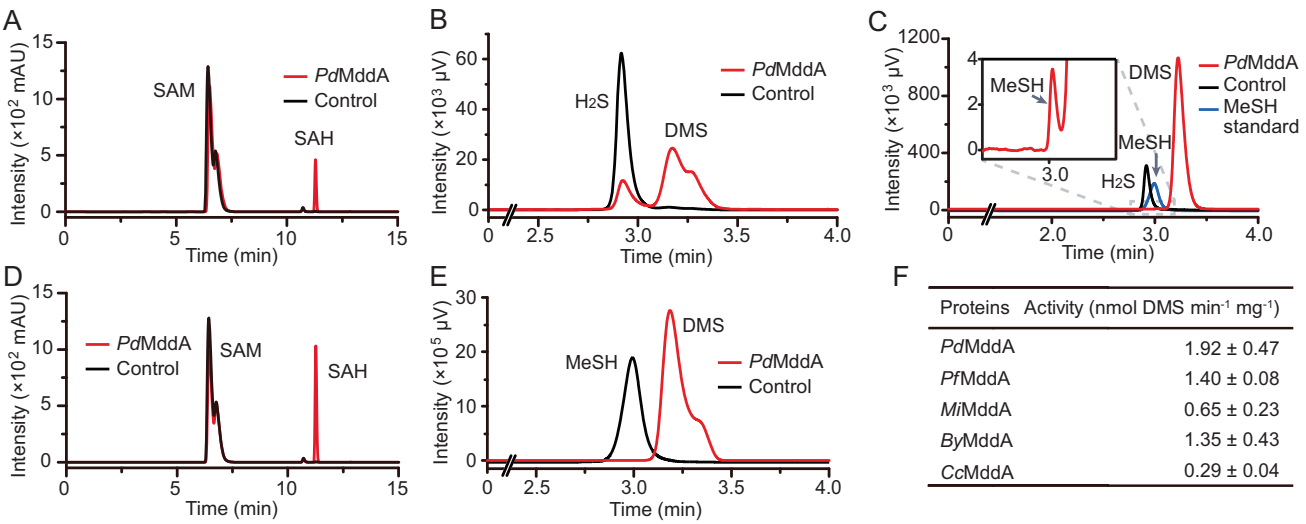

Proteins	Activity (nmol DMS min^{-1} mg^{-1})
*Pd*MddA	1.92 ± 0.47
*Pf*MddA	1.40 ± 0.08
*Mi*MddA	0.65 ± 0.23
*By*MddA	1.35 ± 0.43
*Cc*MddA	0.29 ± 0.04

Fig. 2 Analyses of MddA enzymatic activities. Enzymatic activities of *Pd*MddA using H_2S as the substrate analyzed by HPLC (**A**) and GC (**B**). The reaction mixture contained 1 mM SAM, 4 μg purified MddA and 0.5 mM H_2S. The same reaction mixture but without the addition of *Pd*MddA was used as the control. **C** GC analyses of intermediate MeSH in H_2S methylation process. The peaks of MeSH are indicated by arrows. Enzymatic activity of *Pd*MddA using MeSH as the substrate analyzed by HPLC (**D**) and GC (**E**). The reaction mixture contained 1 mM SAM, 4 μg purified MddA and 0.5 mM MeSH. The same reaction mixture but without the addition of *Pd*MddA was used as the control. **F** Enzymatic activities of MddA homologs using H_2S as the substrate. The MddAs included in the analyses are: *Pd*MddA from *P. deceptionensis* $M1^T$, *Pf*MddA from *P. fragi* (Gammaproteobacteria), *Mi*MddA from *Mycobacterium intracellulare* (Actinobacteria), *By*MddA from *Bradyrhizobium* sp. YR681 (Alphaproteobacteria), *Cc*MddA from *Crocosphaera chwakensis* (cyanobacteria).

Table 1. Kinetic parameters of *Pd*MddA with different substrates.

Substrate	K_m (mM)	k_{cat} (s^{-1})	k_{cat}/K_m ($M^{-1}s^{-1}$)
H_2S	0.41 ± 0.04	7.1×10^{-3}	17.07
MeSH	1.99 ± 0.11	93.0×10^{-3}	46.73
DTT	1.62 ± 0.22	253.3×10^{-3}	156.17
KI	NA[a]	–	–
KSCN	NA[a]	–	–
Captopril	NA[a]	–	–
D-penicillamine	NA[a]	–	–
L-cysteine	NA[a]	–	–
L-homocysteine	NA[a]	–	–
Glutathione	NA[a]	–	–
2-(methylthio)acetic acid	NA[a]	–	–
Thiodiglycolic acid	NA[a]	–	–

[a]No activity detected.

addition to *Pd*MddA, several other purified MddA enzymes from the bacteria known to contain it [18] were also shown to have SAM-dependent *S*-methylation activity on H_2S to produce DMS (Fig. 2F), indicating that the activity of MddA towards H_2S is likely of universal significance to the MddA enzyme family. We noted that in H_2S-dependent DMS production assays of MddA, the levels of MeSH detected were far lower than the DMS product (Fig. 2C). These data support the hypothesis that MddA primarily *S*-methylates H_2S to the intermediate MeSH, which is subsequently *S*-methylated to DMS.

The *Pd*MddA enzyme had an apparent optimum pH of 8.0 and temperature of 30 °C (Supplementary Fig. S1). Thiol *S*-methyltransferases can catalyze the methylation of diverse substrates, including potassium iodide (KI), potassium thiocyanate (KSCN), dithiothreitol (DTT), captopril and D-penicillamine [31, 32, 46]. These compounds, in addition to several cellular thiols (L-cysteine, L-homocysteine, glutathione) and carboxylate substrates (2-(methylthio)acetic acid and thiodiglycolic acid), were used to test the substrate specificity of *Pd*MddA. Of these potential substrates, *Pd*MddA only *S*-methylated H_2S, MeSH and DTT with K_m values of 0.41 mM, 1.99 mM and 1.62 mM, respectively (Table 1 and Supplementary Fig. S2). *Pd*MddA showed notably high k_{cat} and k_{cat}/K_m values towards the artificial substrate DTT which does not accumulate in cells under natural conditions. The concentration of H_2S in natural environments range from several hundred micromolar to several millimolar [25, 26], while MeSH is nanomolar [20]. Thus, H_2S is the only substrate that will likely reach the K_m levels for *Pd*MddA in the environment. *Pd*MddA exhibited a ~5-fold lower K_m value towards the H_2S than for MeSH (Table 1), which was higher than human [32] and rat [29] thiol *S*-methyltransferases but considerably lower than those in plants (Supplementary Table S6). The k_{cat} and k_{cat}/K_m values of *Pd*MddA towards MeSH were higher than for H_2S (Table 1), indicating that the consumption rate of MeSH is likely higher than its production rate. This is consistent with the very low MeSH (intermediate) levels detected in comparison to DMS in H_2S *S*-methylation enzyme assays (Fig. 2C). The higher specific activity of *Pd*MddA towards MeSH than H_2S, may reflect that the reactive gas MeSH is also toxic to cells if allowed to accumulate [47, 48], whereas DMS is not toxic.

Key residues of *Pd*MddA in methylation process

In X-ray crystallography work to elucidate the catalytic mechanism of H_2S-dependent DMS production, we obtained *Pd*MddA crystals but their diffractions were poor, and no structures could be solved. We therefore predicted the structure of *Pd*MddA using AlphaFold2 [36], only analyzing residues R10-S253 that had a > 70 confidence score. *Pd*MddA was predicted to comprise eight main transmembrane helices, with several small helices and two antiparallel β-strands (Fig. 3A).

Analyzing the Protein Data Bank (PDB), *Pd*MddA was most similar to *Tribolium castaneum* isoprenylcysteine carboxyl methyltransferase (*Tc*ICMT, PDB code 5V7P, 27% identity, 33% coverage) and *Methanosarcina acetivorans* isoprenylcysteine carboxyl methyltransferase (*Ma*MTase, PDB code 4A2N, 30% identity, 27% coverage). Despite these low sequence identities, structural alignment showed that the structures of *Pd*MddA, *Tc*ICMT and *Ma*MTase shared four of the eight predicted transmembrane helices (Supplementary Fig. S3). Sequence and structural alignments also showed that five conserved residues (Y185, H190, E228, Y240, Y243) of *Pd*MddA were located near to the SAH molecules of *Ma*MTase and *Tc*ICMT (Fig. 3B, C), suggesting that these residues may participate in SAM binding. Substitution of these residues to alanine significantly decreased the enzymatic activity of *Pd*MddA towards H_2S and MeSH (Fig. 3D, E). Residue H77 of *Pd*MddA, strictly conserved in MddA homologs but not in *Tc*ICMT or *Ma*MTase (Fig. 3C), was located near the sulfur atom of SAH (Fig. 3B). Biochemical analyses showed that substituting H77 to alanine completely abolished the *S*-methyltransferase activity of *Pd*MddA towards both H_2S and MeSH (Fig. 3D, E), implying that H77 could be the catalytic residue.

The *Pd*MddA proposed catalytic mechanism

SAM-dependent methylation is an S_N2 nucleophilic replacement reaction [49, 50]. We predicted the *Pd*MddA catalytic mechanism for H_2S *S*-methylation based on biochemical and structural analyses, which is likely common to all MddA proteins. The *S*-methylation of H_2S can be divided into two steps (Fig. 4A). In the first step, *Pd*MddA binds the SAM and H_2S molecules. H77 acts as a general base and abstracts a proton from the H_2S molecule. The movement of electrons drives the transfer of the methyl group from SAM to the sulfur atom of H_2S, resulting in the formation of MeSH. Subsequently, SAH is released from the active site and a new SAM molecule binds to the active site. The second step is similar to the first step. The residue H77 would become uncharged again in solution, deprotonate the MeSH molecule, and facilitate electron transfer, triggering the methyl transfer from SAM to MeSH, thus enabling the formation of DMS (Fig. 4A). In addition to acting as a base, the residue H77 may also help stabilize the binding of substrate to the active site and retain MeSH at the active site by hydrogen bonding for subsequent conversion to DMS.

Mechanistic informed extension of the MddA enzyme family

With insight into key residues for MddA-driven H_2S and MeSH *S*-methylation, we re-evaluated the occurrence of this enzyme in more diverse organisms. MddA-like proteins with the predicted catalytic H77 and conserved SAM binding residues were identified in many more diverse organisms than were previously reported in Carrión et al. [18], including some chlorophyte (*Pycnococcus provasolii*), diatom (*Nitzschia* sp. RCC80), Chlorarachniophyte (*Lotharella globosa* CCCM811) and Ochraphyta (*Chrysocystis fragilis* CCMP3189) algae and halotolerant archaea (*Haladaptatus* spp.) (Supplementary Fig. S4), not before suspected to produce DMS from H_2S or MeSH. Given that MddA proteins were only thought to exist in diverse bacteria and cyanobacteria, these more diverse candidate MddA enzymes from algae (*P. provasolii*, *Pp*MddA; *N.* sp. RCC80, *Nr*MddA; *L. globose*, *Lg*MddA and *C. fragilis*, *Cf*MddA) and archaea (*Haladaptatus* sp. W1, *Hw*MddA; *Haladaptatus* sp. PSR5, *Hp*MddA) were expressed and purified from *E. coli* and tested for SAM-dependent H_2S S-methylation generating DMS. These proteins all showed *in-vitro* *S*-methylation activity on H_2S and produced DMS (Fig. 4B). By searching homologs of ratified MddA

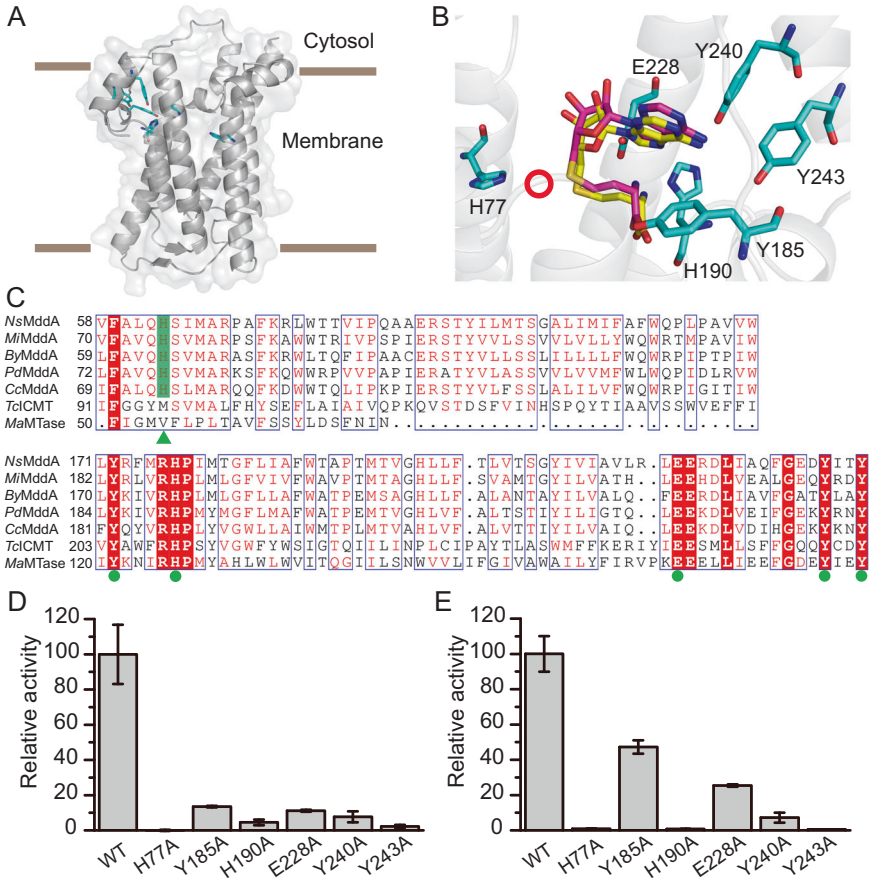

Fig. 3 Important *Pd*MddA residues for enzymatic activity. A The AlphaFold2 predicted structure of *Pd*MddA, with key residues colored in cyan. **B** Key residues of the predicted *Pd*MddA structure. The structures of *Ma*MTase, *Tc*ICMT and *Pd*MddA are superimposed and the SAH molecules of *Ma*MTase and *Tc*ICMT are represented in yellow and magenta, respectively. The residues of *Pd*MddA analyzed in this study are colored in cyan. The potential position of H_2S is indicated by a red circle. **C** Sequence alignment of MddA enzymes and other known methyltransferases. The amino acid sequences included in the alignment are: *Ns*MddA from *N. sediminis*, *Mi*MddA from *M. intracellulare*, *By*MddA from *B.* sp. YR681, *Pd*MddA from *P. deceptionensis* M1^T, *Cc*MddA from *C. chwakensis*, *Tc*ICMT from *T. castaneum* and *Ma*MTase from *M. acetivorans*. The catalytic histidines are indicated with a green triangle. Residues participate in SAM binding are indicated with green dots. **D** Relative activity of wild-type *Pd*MddA and its derivatives with the indicated amino acid substitutions, towards H_2S. The enzymatic activity of wild-type *Pd*MddA towards H_2S is defined as 100%. Data represent the average of three biological replicates with their respective standard deviations. **E** Relative activity of wild-type *Pd*MddA and derived variants on MeSH.

sequences from NCBI NR database and MMETSP (Marine Microbial Eukaryote Transcriptome Sequencing Project) database, we found *mddA* genes are widely distributed in many bacterium phyla (e.g., proteobacteria, acidobacteria and actinobacteria) and several eukaryotic phyla (*Chlorophyta, Bacillariophyta*, *Cercozoa*, and *Rhodophyta*) (Fig. 4C and Supplementary Table S7). These results showed that some diverse algae and archaea likely *S*-methylate H_2S and generate DMS in a DMSP-independent pathway, thus significantly extending the domains of life that conduct this process.

The potential for H_2S-dependent DMS production in diverse environments

Previous research suggested that bacteria with *mddA* are highly abundant (3–77% relative abundance, RA) in diverse soils, rhizosphere and surface saltmarsh sediment environments, but extremely scarce (0.01% RA) in marine water samples [17, 18, 22]. This led to the prediction that MeSH-, and now H_2S-dependent DMS production was likely a significant process in sediment environments but insignificant in marine environments [17, 18, 22]. As this study significantly extended the suite and diversity organisms known to contain a functional *mddA* gene, we re-examined the importance of *mddA* in more diverse marine settings in comparison to the most abundant DMSP lyase gene *dddP*.

Analysis of metagenomes from diverse environments confirmed previous work by showing *mddA* to be far more abundant in marine or terrestrial sediments than in diverse seawater or freshwater samples (Fig. 5A). In addition, it was clear that *mddA* in hydrothermal vents was also abundant (Fig. 5A). This was not surprising given H_2S is naturally abundant in many sediment and hydrothermal vent environments [24–26]. The previously held prediction that MeSH- and now H_2S-dependent DMS production, was an important process in sediment environments is strongly supported here. Compared to *dddP*, *mddA* was less abundant in most of our examined environments, except for lake sediment and soil environments (Fig. 5A). Within marine water samples, eukaryotic *Alma1* and bacterial *dddP* DMSP lyase gene sequences and transcripts were more abundant than their *mddA* equivalents (Supplementary Fig. S5A, B). These data imply that MddA-driven DMS production is a considerable, although may not be the major, source of DMS in H_2S-rich environments (Fig. 5B).

It was difficult to resolve the taxonomy of many of the prokaryotic *mddA* genes beyond the bacterial domain and Proteobacterial phylum in most metagenomic samples (see Supplementary Fig. S5 for marine samples). The marine eukaryotic *mddA* genes were more easily assigned and were affiliated to *Chlorophyta*, *Cercozoa* and *Bacillariophyta* or, unexpectedly, more than half of these sequences were from *Appendicularia*, a group of

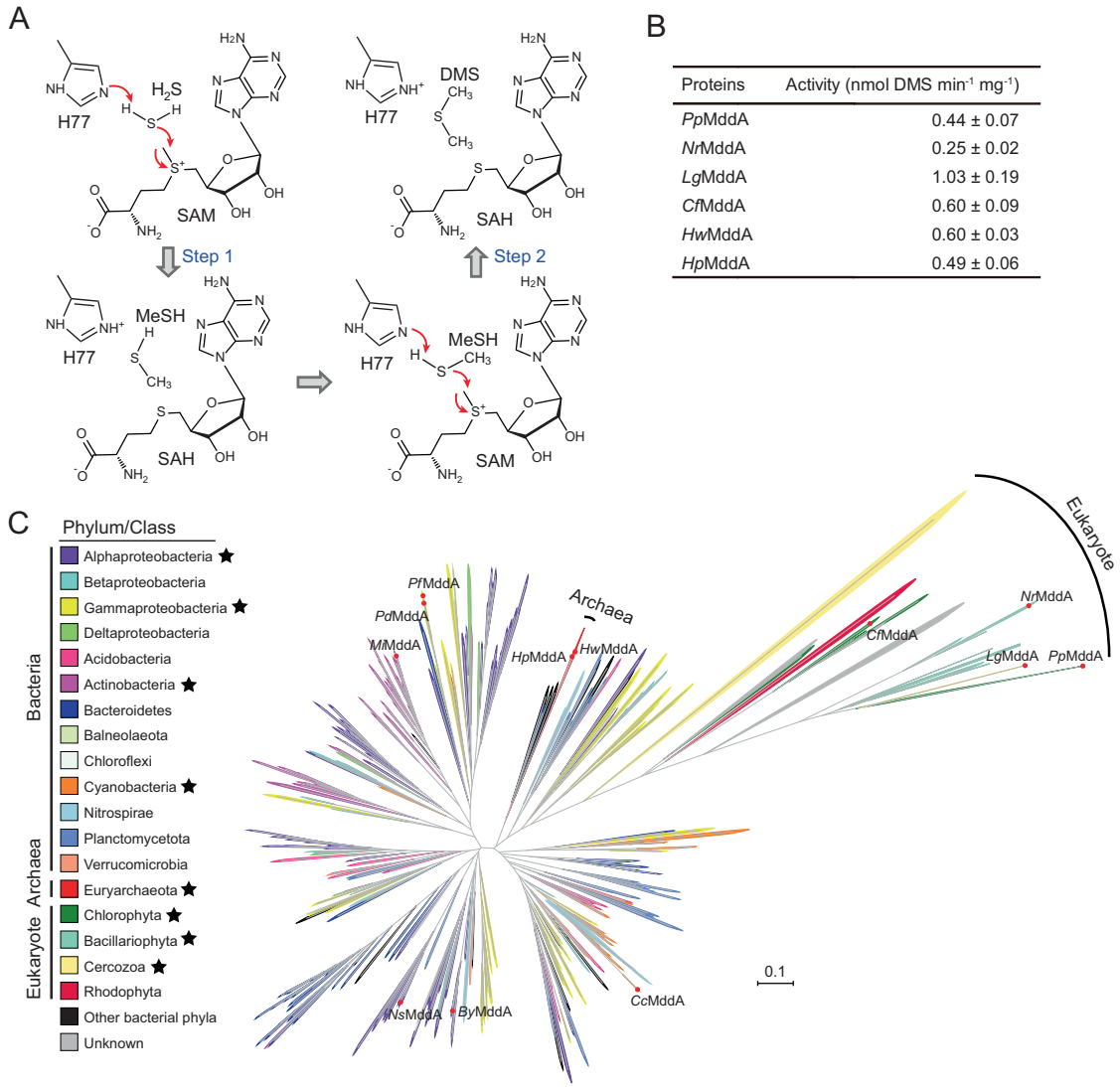

Proteins	Activity (nmol DMS min^{-1} mg^{-1})
*Pp*MddA	0.44 ± 0.07
*Nr*MddA	0.25 ± 0.02
*Lg*MddA	1.03 ± 0.19
*Cf*MddA	0.60 ± 0.09
*Hw*MddA	0.60 ± 0.03
*Hp*MddA	0.49 ± 0.06

Fig. 4 The predicted catalytic mechanism of MddA and the enzymatic activities of MddA-like proteins in algae and archaea. A The proposed catalytic mechanism of H_2S methylation by *Pd*MddA. Putative electron transfers are indicated by red arrows. **B** Enzymatic activities of MddA-like proteins in algae and archaea. The MddA-like proteins included in the analyses are: *Pp*MddA from *P. provasolii* (chlorophyte algae), *Nr*MddA from *N.* sp. RCC80, *Lg*MddA from *Lotharella globosa* CCCM811, *Cf*MddA from *C. fragilis* CCMP3189, *Hw*MddA from *Haladaptatus* sp. W1 (halotolerant archaea), *Hp*MddA from *Haladaptatus* sp. PSR5 (halotolerant archaea). The same reaction mixture without the addition of enzyme was used as negative control. **C** Distribution of MddA in bacteria, archaea and eukaryotes. Branches are colored according to their taxonomic affiliations at phylum or class level. All ratified MddA sequences are marked in red solid circles. The dark stars are used to mark phylum containing ratified MddA. Tree scale indicates evolutionary distance as rate of substitution per site. The scale bar corresponds to 0.1.

solitary and free-swimming tunicates found throughout the world's oceans (Supplementary Fig. S5C, D). The *Appendicularia* had not previously been linked to DMS production whatsoever.

Role for MddA in detoxification of H_2S

H_2S is a toxic compound, whereas, to our knowledge, DMS is not harmful to organisms. Thus, the MddA-driven conversion of H_2S to DMS may be a cellular detoxification strategy. To test this hypothesis, we examined the growth characteristics of wild type *N. sediminis* Δ*mddA* strain in the presence of H_2S. Growth of the Δ*mddA* mutant was significantly impaired by the addition of 2 mM H_2S compared to the wild type strains and this phenotype was fully complemented by cloned *mddA* (Fig. 6A, B). In addition to work in *N. sediminis*, we also performed growth inhibition work in *E. coli* expressing MddA. The growth of *E. coli* in the presence of 2 mM H_2S was enhanced by the expression of MddA (Fig. 6C, D). These data indicate that MddA plays a role in detoxification of H_2S in diverse organisms and environments.

DISCUSSION

H_2S and DMS are abundant and important forms of inorganic and organic sulfur, respectively, in natural environments. The *S*-methylation of H_2S to DMS via MeSH represents a biological route from inorganic to organic sulfur (Fig. 5B). H_2S readily reacts with metal ions to produce metal sulfides, can be oxidized to thiosulfate by dissolved organic matter in sediments [51], and is highly toxic to cells by virtue of inhibiting cytochrome *c* oxidase activity electron transport chains [27, 28]. In contrast, DMS is relatively stable in environments and is non-toxic to cells [52]. The majority of DMS in the environment is degraded by microbial or, to a lesser extent, photochemical processes [52]. Some bacteria utilize DMS as a source of reduced carbon and/or sulfur and/or energy [53]. Therefore, through the methylation of H_2S, some bacteria (not necessarily those generating the DMS via MddA) can incorporate sulfur from H_2S into organic matter necessary for growth.

Several thiol *S*-methyltransferase enzymes that catalyze H_2S methylation to DMS had been identified in higher animals and

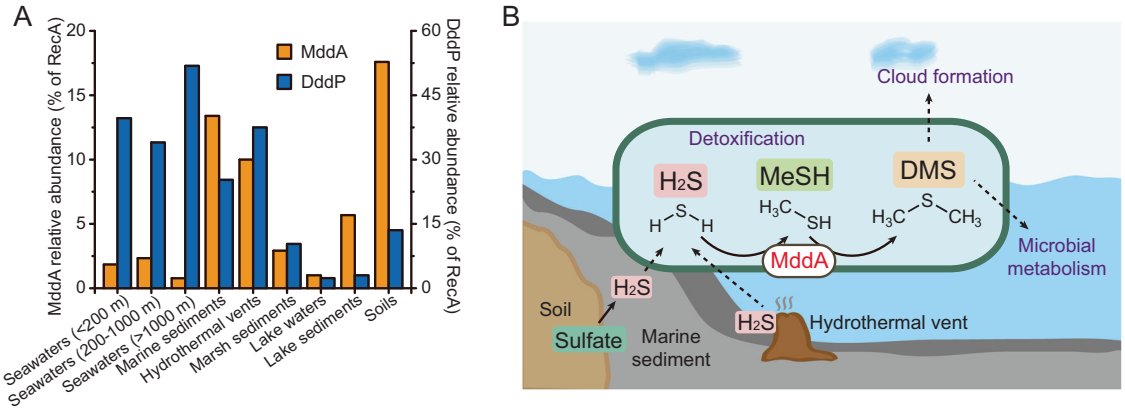

Fig. 5 MddA mediated H_2S *S*-methylation in natural environments. A Relative abundance of MddA and DddP protein-encoding sequences in different environmental metagenomes. The numbers of MddA and DddP sequences were normalized to the number of RecA sequences in each metagenome. **B** Diagram of H_2S methylation mediated by aerobic bacteria. Sulfate is transformed into H_2S by sulfate-reducing microorganisms in soil and marine sediments. H_2S can also be directly released from oceanic crust through hydrothermal vents. H_2S from both terrestrial environments and marine environments can be methylated to MeSH then to DMS, which act as a detoxification process.

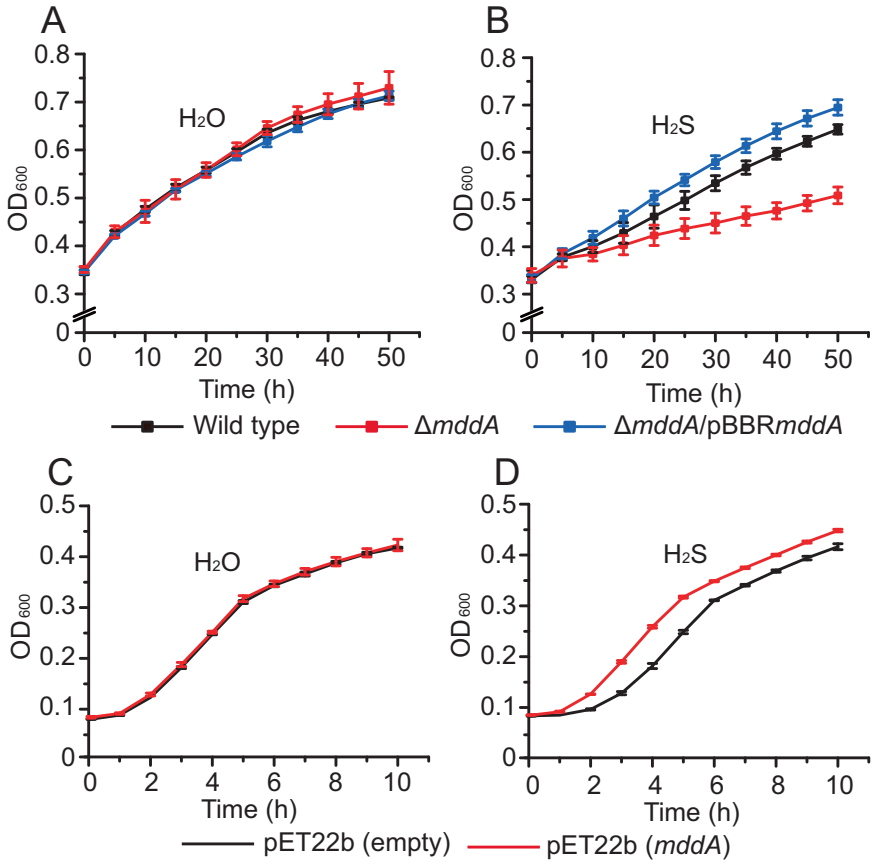

Fig. 6 Growth of *N. sediminis* and *E. coli* in response to H_2S. A Growth of *N. sediminis* strains with H_2O (control). **B** Growth of *N. sediminis* strains in the presence of H_2S. **C** Growth of *E. coli* with H_2O added (control). **D** Growth curve of *E. coli* strains amended with H_2S. H_2S was used at 1 mM final concentration. Values shown represent the average of three biological replicates with their respective standard deviations.

plants [29, 31, 32], but to the best of our knowledge, there had been no aerobic bacteria, archaea or algae reported to have this activity. Our data showed that many and diverse organisms including aerobic bacteria and, likely, archaea and photosynthetic bacteria, and algae, *S*-methylate H_2S to produce DMS via the MddA *S*-methyltransferase for protection against the cellular toxicity of H_2S and potentially MeSH.

MddA is located in the cell membrane, which may be important for bacteria to respond to H_2S toxicity since it was reported that no channels or facilitators were needed for H_2S to permeate cell membranes [54, 55]. Therefore, environmental H_2S gas can easily enter the cell. The partition coefficient of H_2S between membrane and water is ~2, and thus, H_2S concentration in the membrane would be higher than the concentration in cytosol [55, 56]. In addition, terminal oxidases in cellular respiration such as cytochrome *c* oxidase and cytochrome bo_3 oxidase, which H_2S inhibits, are also membranous enzymes. In addition to detoxification, *S*-methylation of H_2S to DMS may also play other

physiological roles. For example, the DMS produced from H_2S *S*-methylation may act as a sulfur and/or an energy source for some bacteria [57–59]; DMS and/or its oxidation product DMSO [60] may serve as antioxidants to protect against oxidative stress [61]; or DMS could act as chemical signaling molecule to attract or deter grazers [1, 62].

H_2S *S*-methylation to yield DMS was previously observed in anoxic freshwater sediments [20]. Furthermore, previous research showed that grassland and forest soils, and saltmarsh sediment samples displayed MeSH-dependent DMS production [17, 18]. Here, we demonstrate that diverse soil, marine and lake sediments, and seawater samples display significant levels of H_2S-dependent DMS production. H_2S-dependent DMS production is likely more prominent than suggested from our examination of environmental omics datasets because many organisms exhibiting MeSH and/or H_2S-dependent DMS production phenotypes contain unknown enzymes with these activities since their genomes lack *mddA* [17] or they contain multiple different enzymes with these activities, as was predicted for *N. sediminis*. It will be important to identify these enzymes in the future to better evaluate the environmental significance of H_2S- and MeSH-dependent DMS production.

The data presented here imply that both eukaryotic and prokaryotic MddA-driven H_2S and/or MeSH-dependent DMS production pathways are important in aquatic and marine settings, but that their importance vastly increases in marine and terrestrial sediment and hydrothermal vent settings where *mddA* sequences can be relatively abundant. Considering that H_2S is abundant in various environments and our re-evaluation of the abundance of *mddA* in diverse organisms and environments, the significance of MddA in global DMS production influencing atmospheric chemistry and potentially climate, and sulfur cycling has been previously underestimated.

DATA AVAILABILITY

The predicted structure can be obtained from the AlphaFold Protein Structure Database (https://alphafold.ebi.ac.uk/) with accession code A0A0F6P9C0. The sequences of MddA and other proteins can be found in NCBI database as well as Supplementary Information files.

REFERENCES

1. Shemi A, Alcolombri U, Schatz D, Farstey V, Vincent F, Rotkopf R, et al. Dimethyl sulfide mediates microbial predator-prey interactions between zooplankton and algae in the ocean. Nat Microbiol. 2021;6:1357–66.
2. De Zwart JMM, Kuenen JG. C1-cycle of sulfur compounds. Biodegradation. 1992;3:37–59.
3. Charlson RJ, Lovelock JE, Andreae MO, Warren SG. Oceanic phytoplankton, atmospheric sulfur, cloud albedo and climate. Nature. 1987;326:655–61.
4. Quinn PK, Bates TS. The case against climate regulation via oceanic phytoplankton sulphur emissions. Nature. 2011;480:51–6.
5. Kettle AJ, Andreae MO. Flux of dimethylsulfide from the oceans: a comparison of updated data seas and flux models. J Geophys Res Atmos. 2000;105:26793–808.
6. Watts SF. The mass budgets of carbonyl sulfide, dimethyl sulfide, carbon disulfide and hydrogen sulfide. Atmos Environ. 2000;34:761–79.
7. Vallina SM, Simo R. Strong relationship between DMS and the solar radiation dose over the global surface ocean. Science. 2007;315:506–8.
8. Curson ARJ, Liu J, Martinez AB, Green RT, Chan YH, Carrion O, et al. Dimethylsulfoniopropionate biosynthesis in marine bacteria and identification of the key gene in this process. Nat Microbiol. 2017;2:17009.
9. Curson AR, Todd JD, Sullivan MJ, Johnston AW. Catabolism of dimethylsulphoniopropionate: microorganisms, enzymes and genes. Nat Rev Microbiol. 2011;9:849–59.
10. Yoch DC. Dimethylsulfoniopropionate: Its sources, role in the marine food web, and biological degradation to dimethylsulfide. Appl Environ Microbiol. 2002;68:5804–15.
11. Alcolombri U, Ben-Dor S, Feldmesser E, Levin Y, Tawfik DS, Vardi A. Identification of the algal dimethyl sulfide-releasing enzyme: A missing link in the marine sulfur cycle. Science. 2015;348:1466–9.
12. Li CY, Wang XJ, Chen XL, Sheng Q, Zhang S, Wang P, et al. A novel ATP dependent dimethylsulfoniopropionate lyase in bacteria that releases dimethyl sulfide and acryloyl-CoA. eLife. 2021;10:e64045.
13. Kiene RP, Hines ME. Microbial formation of dimethyl sulfide in anoxic sphagnum peat. Appl Environ Microbiol. 1995;61:2720–6.
14. Zinder SH, Brock TD. Dimethyl sulphoxide reduction by micro-organisms. J Gen Microbiol. 1978;105:335–42.
15. Spiese CE, Kieber DJ, Nomura CT, Kiene RP. Reduction of dimethylsulfoxide to dimethylsulfide by marine phytoplankton. Limnol Oceanogr. 2009;54:560–70.
16. Stets EG, Hines ME, Kiene RP. Thiol methylation potential in anoxic, low-pH wetland sediments and its relationship with dimethylsulfide production and organic carbon cycling. FEMS Microbiol Ecol. 2004;47:1–11.
17. Carrion O, Pratscher J, Curson ARJ, Williams BT, Rostant WG, Murrell JC, et al. Methanethiol-dependent dimethylsulfide production in soil environments. ISME J. 2017;11:2379–90.
18. Carrion O, Curson AR, Kumaresan D, Fu Y, Lang AS, Mercade E, et al. A novel pathway producing dimethylsulphide in bacteria is widespread in soil environments. Nat Commun. 2015;6:6579.
19. Reisch CR, Stoudemayer MJ, Varaljay VA, Amster IJ, Moran MA, Whitman WB. Novel pathway for assimilation of dimethylsulphoniopropionate widespread in marine bacteria. Nature. 2011;473:208–11.
20. Lomans BP, Smolders AJP, Intven LM, Pol A, denCamp HJMO, vanderDrift C. Formation of dimethyl sulfide and methanethiol in anoxic freshwater sediments. Appl Environ Microbiol. 1997;63:4741–7.
21. Bak F, Finster K, Rothfuss F. Formation of dimethylsulfide and methanethiol from methoxylated aromatic compounds and inorganic sulfide by newly isolated anaerobic bacteria. Arch Microbiol. 1992;157:529–34.
22. Carrion O, Pratscher J, Richa K, Rostant WG, Ul Haque MF, Murrell JC, et al. Methanethiol and dimethylsulfide cycling in stiffkey saltmarsh. Front Microbiol. 2019;10:1040.
23. Andreae MO. Ocean-atmosphere interactions in the global biogeochemical sulfur cycle. Mar Chem. 1990;30:1–29.
24. Bagarinao T. Sulfide as an environmental factor and toxicant: tolerance and adaptations in aquatic organisms. Aquat Toxicol. 1992;24:21–62.
25. Johnson KS, Beehler CL, Sakamoto-Arnold CM, Childress JJ. In situ measurements of chemical distributions in a deep-sea hydrothermal vent field. Science 1986;231:1139–41.
26. Thompson BE, Bay SM, Anderson JW, Laughlin JD, Greenstein DJ, Tsukada DT. Chronic effects of contaminated sediments on the urchin Lytechinus pictus. Environ Toxicol Chem. 1989;8:629–37.
27. Malone Rubright SL, Pearce LL, Peterson J. Environmental toxicology of hydrogen sulfide. Nitric Oxide. 2017;71:1–13.
28. Cuevasanta E, Moller MN, Alvarez B. Biological chemistry of hydrogen sulfide and persulfides. Arch Biochem Biophys. 2017;617:9–25.
29. Weisiger RA, Pinkus LM, Jakoby WB. Thiol S-methyltransferase: suggested role in detoxication of intestinal hydrogen sulfide. Biochem Pharm. 1980;29:2885–7.
30. Sun Y, Wang M, Zhong Z, Chen H, Wang H, Zhou L, et al. Adaption to hydrogen sulfide-rich environments: Strategies for active detoxification in deep-sea symbiotic mussels, *Gigantidas platifrons*. Sci Total Environ. 2022;804:150054.
31. Itoh N, Toda H, Matsuda M, Negishi T, Taniguchi T, Ohsawa N. Involvement of *S*-adenosylmethionine-dependent halide/thiol methyltransferase (HTMT) in methyl halide emissions from agricultural plants: isolation and characterization of an HTMT-coding gene from *Raphanus sativus* (daikon radish). BMC Plant Biol. 2009;9:116.
32. Maldonato BJ, Russell DA, Totah RA. Human METTL7B is an alkyl thiol methyltransferase that metabolizes hydrogen sulfide and captopril. Sci Rep. 2021;11:4857.
33. Sambrook J, Russell DW. Molecular cloning, a laboratory manual. 3rd ed. New York, USA: Cold Spring Harbor Laboratory Press; 2001.
34. Wang PX, Yu ZC, Li BY, Cai XS, Zeng ZS, Chen XL, et al. Development of an efficient conjugation-based genetic manipulation system for *Pseudoalteromonas*. Micro Cell Fact. 2015;14:11.
35. Kovach ME, Elzer PH, Hill DS, Robertson GT, Farris MA, Roop RM, et al. Four new derivatives of the broad-host-range cloning vector pBBR1MCS, carrying different antibiotic-resistance cassettes. Gene. 1995;166:175–6.
36. Jumper J, Evans R, Pritzel A, Green T, Figurnov M, Ronneberger O, et al. Highly accurate protein structure prediction with AlphaFold. Nature. 2021;596:583–9.
37. Varadi M, Anyango S, Deshpande M, Nair S, Natassia C, Yordanova G, et al. AlphaFold Protein Structure Database: massively expanding the structural coverage of protein-sequence space with high-accuracy models. Nucleic Acids Res. 2022;50:D439–D44.
38. Fu LM, Niu BF, Zhu ZW, Wu ST, Li WZ. CD-HIT: accelerated for clustering the next-generation sequencing data. Bioinformatics 2012;28:3150–2.
39. Katoh K, Rozewicki J, Yamada KD. MAFFT online service: multiple sequence alignment, interactive sequence choice and visualization. Brief Bioinform. 2019;20:1160–6.
40. Capella-Gutierrez S, Silla-Martinez JM, Gabaldon T. trimAl: a tool for automated alignment trimming in large-scale phylogenetic analyses. Bioinformatics 2009;25:1972–3.

41. Price MN, Dehal PS, Arkin AP. FastTree 2-approximately maximum-likelihood trees for large alignments. PLoS One. 2010;5:e9490.
42. Letunic I, Bork P. Interactive Tree Of Life (iTOL) v5: an online tool for phylogenetic tree display and annotation. Nucleic Acids Res. 2021;49:W293–W6.
43. Vernette C, Lecubin J, Sanchez P, Tara Oceans C, Sunagawa S, Delmont TO, et al. The Ocean Gene Atlas v2.0: online exploration of the biogeography and phylogeny of plankton genes. Nucleic Acids Res. 2022;50:W516–26.
44. Chen IA, Chu K, Palaniappan K, Ratner A, Huang J, Huntemann M, et al. The IMG/M data management and analysis system v.6.0: new tools and advanced capabilities. Nucleic Acids Res. 2021;49:D751–D63.
45. Zhang YJ, Liu XF, Kuang BZ, Zhang XY, Zhou MY, Chen S. *Neptunicoccus sediminis* gen. nov., sp. nov., a member of the family *Rhodobacteraceae* isolated from the Yellow Sea. Int J Syst Evol Microbiol. 2018;68:1702–6.
46. Toda H, Itoh N. Isolation and characterization of a gene encoding a *S*-adenosyl-L-methionine-dependent halide/thiol methyltransferase (HTMT) from the marine diatom *Phaeodactylum tricornutum*: Biogenic mechanism of CH3I emissions in oceans. Phytochemistry 2011;72:337–43.
47. Furne J, Springfield J, Koenig T, DeMaster E, Levitt MD. Oxidation of hydrogen sulfide and methanethiol to thiosulfate by rat tissues: a specialized function of the colonic mucosa. Biochem Pharm. 2001;62:255–9.
48. Wirth JS, Wang T, Huang QY, White RH, Whitman WB. Dimethylsulfoniopropionate sulfur and methyl carbon assimilation in *Ruegeria* species. mBio. 2020;11:e00329-20.
49. Liscombe DK, Louie GV, Noel JP. Architectures, mechanisms and molecular evolution of natural product methyltransferases. Nat Prod Rep. 2012;29:1238–50.
50. Sun Q, Huang MY, Wei YQ. Diversity of the reaction mechanisms of SAM-dependent enzymes. Acta Pharmaceutica Sin B. 2021;11:632–50.
51. Tobias H, Christian B. Oxidation and incorporation of hydrogen sulfide by dissolved organic matter. Chem Geol. 2006;235:12–20.
52. Kiene RP, Bates TS. Biological removal of dimethyl sulfide from sea-water. Nature. 1990;345:702–5.
53. Kappler U, Schafer H. Transformations of dimethylsulfide. Met Ions Life Sci. 2014;14:279–313.
54. Mathai JC, Missner A, Kugler P, Saparov SM, Zeidel ML, Lee JK, et al. No facilitator required for membrane transport of hydrogen sulfide. Proc Natl Acad Sci USA. 2009;106:16633–8.
55. Riahi S, Rowley CN. Why can hydrogen sulfide permeate cell membranes? J Am Chem Soc. 2014;136:15111–3.
56. Cuevasanta E, Denicola A, Alvarez B, Moller MN. Solubility and permeation of hydrogen sulfide in lipid membranes. PLoS One. 2012;7:e34562.
57. Horinouchi M, Kasuga K, Nojiri H, Yamane H, Omori T. Cloning and characterization of genes encoding an enzyme which oxidizes dimethyl sulfide in *Acinetobacter* sp. strain 20B. FEMS Microbiol Lett. 1997;155:99–105.
58. Fuse H, Takimura O, Murakami K, Yamaoka Y, Omori T. Utilization of dimethyl sulfide as a sulfur source with the aid of light by *Marinobacterium* sp. strain DMS-S1. Appl Environ Microbiol. 2000;66:5527–32.
59. Boden R, Murrell JC, Schafer H. Dimethylsulfide is an energy source for the heterotrophic marine bacterium *Sagittula stellata*. FEMS Microbiol Lett. 2011;322:188–93.
60. Lidbury I, Krober E, Zhang ZD, Zhu YJ, Murrell JC, Chen Y, et al. A mechanism for bacterial transformation of dimethylsulfide to dimethylsulfoxide: a missing link in the marine organic sulfur cycle. Environ Microbiol. 2016;18:2754–66.
61. Sunda W, Kieber DJ, Kiene RP, Huntsman S. An antioxidant function for DMSP and DMS in marine algae. Nature. 2002;418:317–20.
62. Teng ZJ, Wang P, Chen XL, Guillonneau R, Li CY, Zou SB, et al. Acrylate protects a marine bacterium from grazing by a ciliate predator. Nat Microbiol. 2021;6:1351–6.

ACKNOWLEDGEMENTS

We thank Terry McGenity from University of Essex for providing the *Haladaptatus* sp. W1 strain, and Emese Bartha from University of East Anglia for providing advice on how to culture it. This work was supported by the Marine S&T Fund of Shandong Province for Qingdao Marine Science and Technology Center (No. 2022QNLM030004-3), the National Key Research and Development Program of China (2022YFC2807500), the National Science Foundation of China (grants 42276102, 92251303, 42076229, 31961133016), the Fundamental Research Funds for the Central Universities (202172002, 202041011), the Major Scientific and Technological Innovation Project (MSTIP) of Shandong Province (2019JZZY010817), the Program of Shandong for Taishan Scholars (tspd20181203), the Biotechnology and Biological Sciences Research Council, UK, grant (BB/X005968), Natural Environment Research Council, UK, Standard grants (NE/X000990, NE/V000756 and NE/S001352) and the Leverhulme Trust research grant (RPG-2020-413).

AUTHOR CONTRIBUTIONS

CYL and YZZ designed and directed the research. JDT designed some experiments. HYC, CYL, QW, OC, XZ and JM performed the experiments. PW, XZ and XLC helped in data analysis. HYC, CYL, JDT and YZZ wrote the manuscript. XLC edited the manuscript.

COMPETING INTERESTS

The authors declare no competing interests.

ADDITIONAL INFORMATION

Supplementary information The online version contains supplementary material available at https://doi.org/10.1038/s41396-023-01430-z.

Correspondence and requests for materials should be addressed to Hai-Yan Cao or Yu-Zhong Zhang.